Application of Artificial Neural Network for Assisting Seismic-Based Reservoir Characterization

by

Bambang Widarsono, Fakhriyadi Saptono, Patrick M. Wong, and **Suprajitno Munadi,**

ABSTRACT

Reservoir rock physical properties, such as porosity and water saturation, always play prominent roles in the development of oil and gas fields. Accurate information regarding their distribution is always desired. For this purpose, a new approach that uses a combination of intelligent computing (artificial neural network or ANN) and rock physics, with a full utilization of core data, well logs and seismic-derived attributes, is proposed. The method is basically an effort to link the required rock physical properties to seismic-derived attributes through the use of rock physics theories. The ANN itself is used to fill the gaps of data array required by the proposed method through its capacity for pattern recognition. The proposed method is applied to a limestone reservoir in East Java. Validation is carried out by comparing the results to the observed data at well locations as well as by geological justification. The application has shown a new potential for supporting reservoir modeling and field development.

I. INTRODUCTION

An important factor in the reliability of a reservoir model is the level of uncertainty in the reservoir characterization stage. Various efforts have been made in order to reduce the uncertainty level. Current developments in reservoir characterization have given much attention to integrating results from seismic data. In other words, the main objective is to extract as much information as possible from seismic surveys. Use of seismic data is now beyond exploration activities and construction of reservoir structure. Recent advances of seismic inversion have facilitated exploration toward extracting rock physical properties for building reservoir simulation models (e.g. Furre and Brevik, 2000; Vidal et al., 2000).

The introduction of statistical pattern recognition (artificial neural network, ANN) in reservoir characterization has the potential for further reducing the uncertainty of reservoir predictions. Recent work by Mukerji et al. (2001) attempts to integrate rock physics, statistical pattern recognition, seismic inversion, and geostatistics in order to map the distribution of lithofacies and fluid contents. In general they apply a Bayesian statistical classification for grouping seismic attributes for lithofacies and fluid contents, as well as their corresponding iso-probability surfaces. For spatial correlation, geostatistical techniques (stochastic simulation) are used.

Following a similar approach this paper introduces a methodology for combining the strengths of both ANN and rock physics for improved porosity and water saturation predictions from core data, well logs and seismic-derived properties. The methodology is applied to a heterogeneous oil producing limestone reservoir (EJ field) in Indonesia.

II. AN INTEGRATED TECHNIQUE

Widarsono and Saptono (1997, 2000a, 2000b, and 2001) propose a technique for preparing log and core data for the purpose of extracting porosity and water saturation from seismic attributes. Following its application on real seismic data (Widarsono et al., 2001), the proposed technique is best performed in the following steps:

1. Measurement of porosity, water saturation, density, P-wave and S-wave velocities, and the determination of rock mechanical properties.
2. Modeling of the relationships between physical properties (e.g. porosity and water saturation),

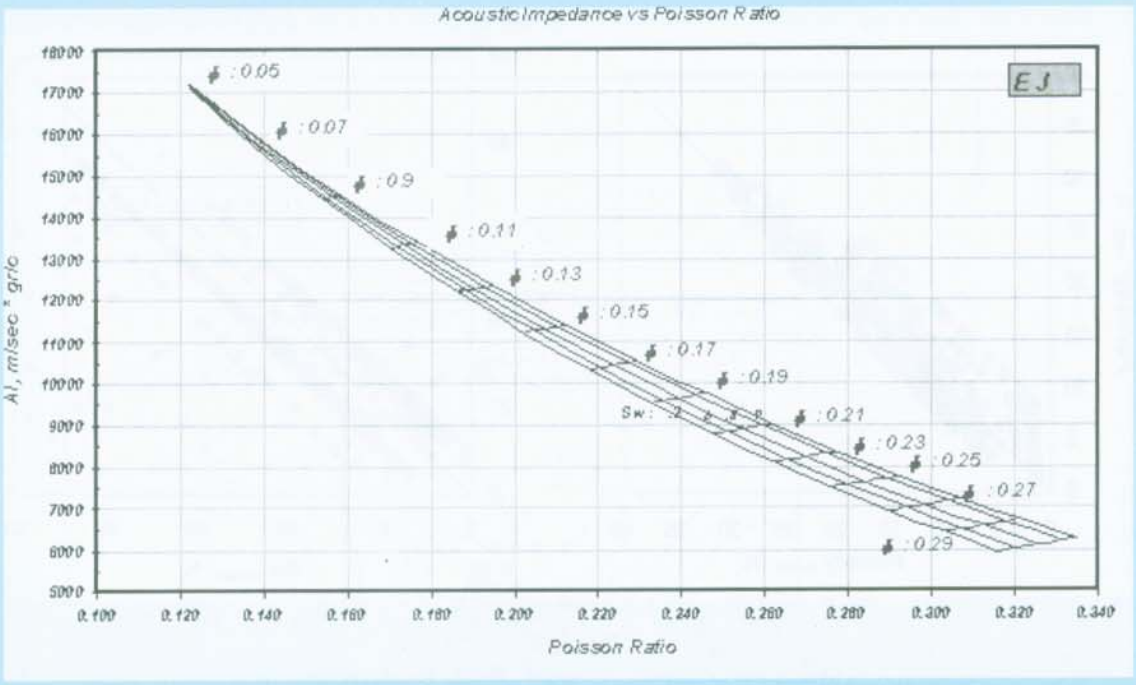

Figure 1
Model relationship for measured data from core samples

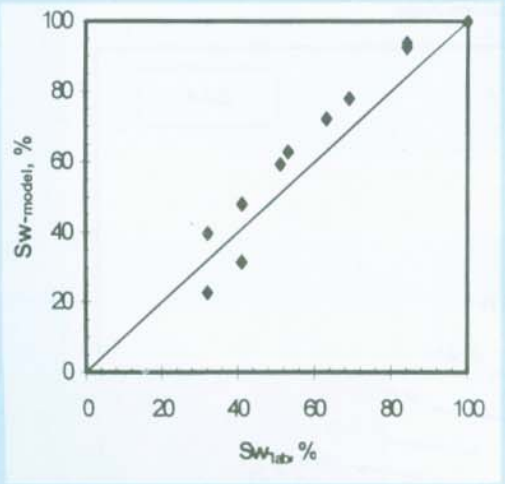

Figure 2
Evidence of validity for water saturation (core data)

P-wave velocity and Poisson ratio using a combination of Gassmann acoustic velocity model (Gassmann, 1951) and the theory of elastic wave propagation (Figure 1-presents a typical example of the model).

3. Model validation through comparing, involving iteration, both model and observed porosity and water saturation values (an example for water saturation is shown in Figure 2). The 'effective' rock matrix bulk and shear modulus used in the validated model is then used in the modeling on well log data as 'first guess' values.
4. Similar modeling on well log data (preferentially done on key wells that have the most complete sets of data) taking into accounts the effect of variations in density and shale contents. Adjustment of the 'first guess' rock matrix data is made on the line of comparing porosity and water saturation between model and log data. Poisson ratio and acoustic impedance data is used as input for the model. See Widarsono et al. (2001) for the method for generating synthetic poisson ratio from log data. An example for the model validity is presented in Figure 3.
5. Confirmation and validation following step 4, which results in the modeled relation, are ready to be used to interpret seismic attributes. An example of the relation (in the form of a cross-plot) is presented in Figure 4.
6. Application of spatial correlation, whether deterministic or stochastic, on seismic attributes. The seismic

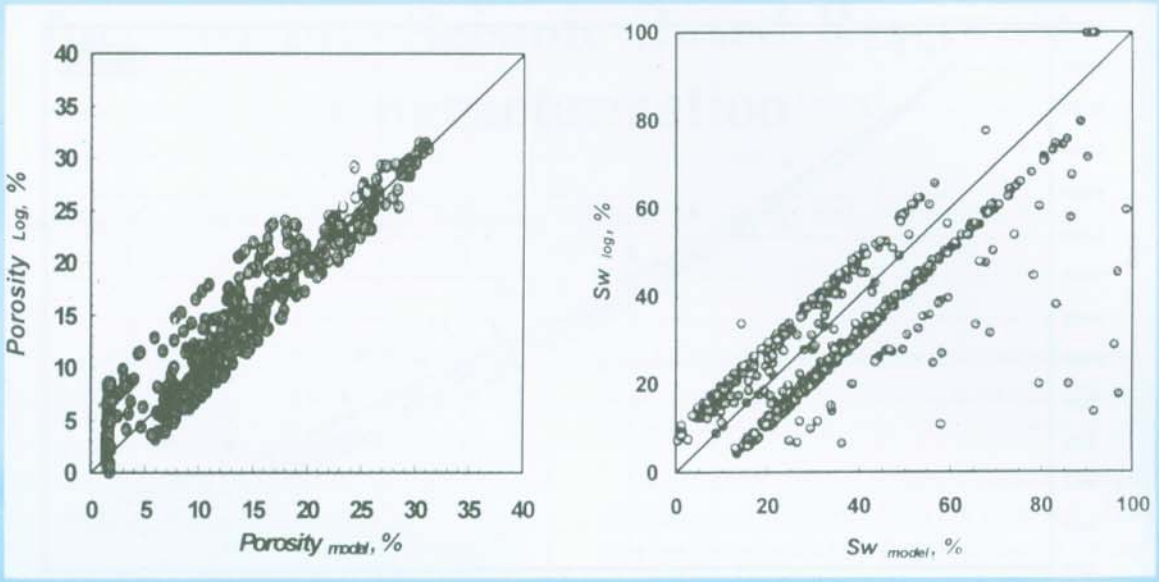

Figure 3
(a and b). Evidence of model validity for log data

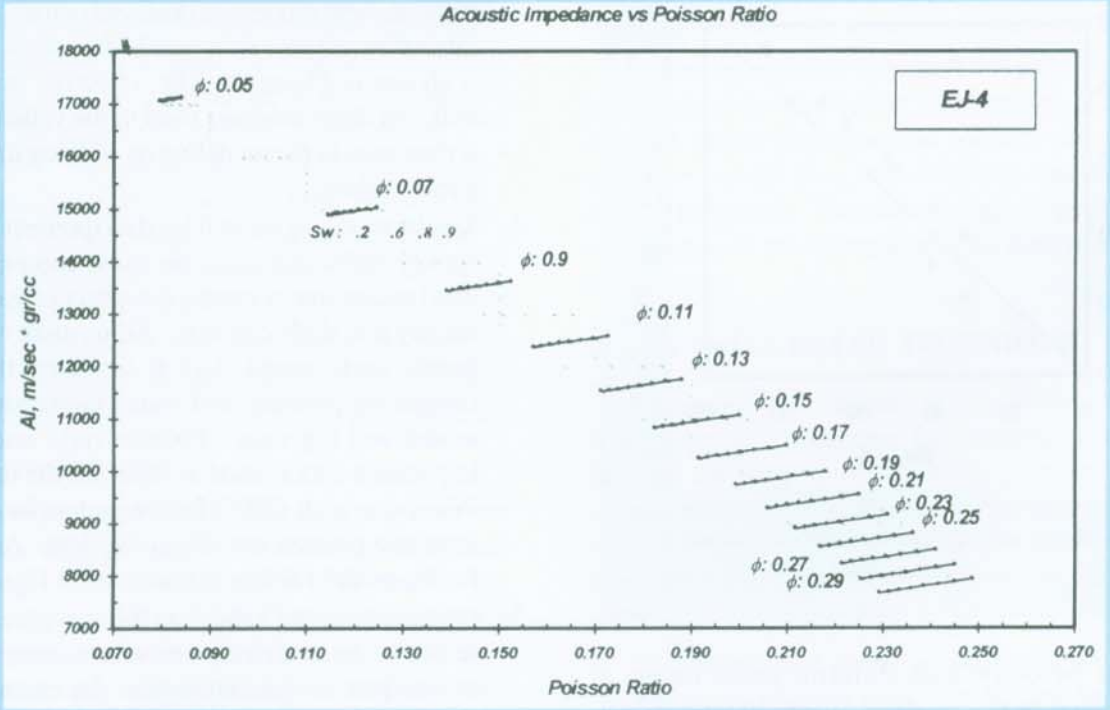

Figure 4
Examples of the model relationship for *in situ* condition

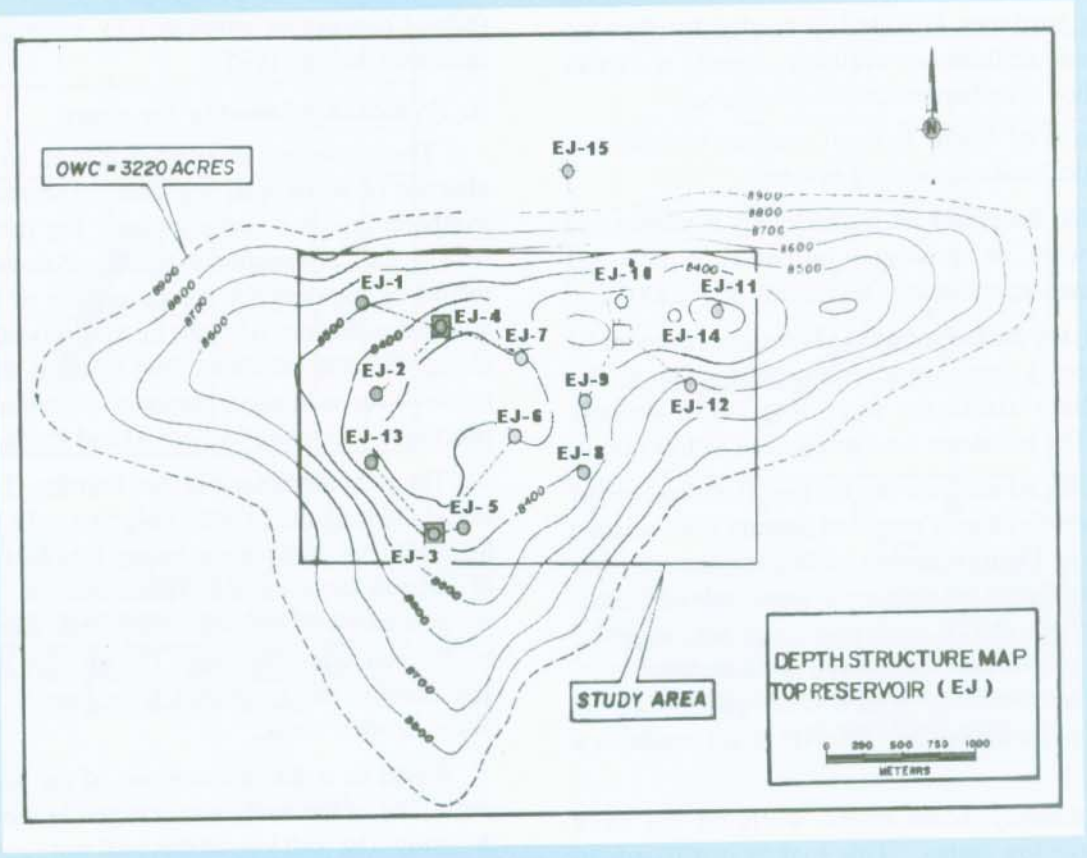

Figure 5
Depth structure map of EJ

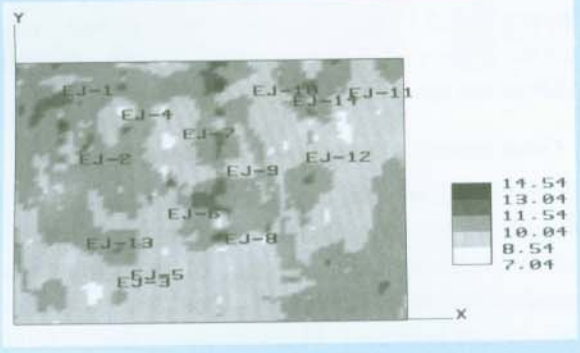

Figure 6
Acoustic impedance map for the top 10 milliseconds (30 – 40 ft thick) interval

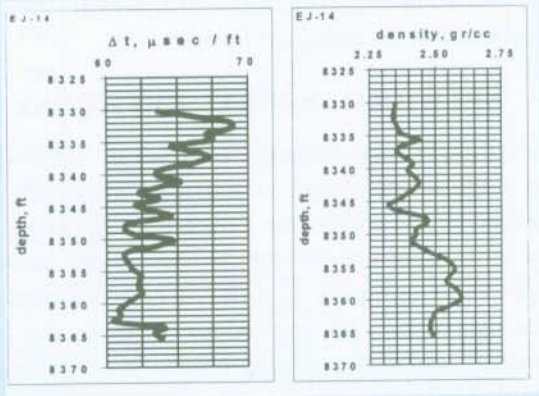

Figure 7
Examples of predicted sonic and density logs (EJ-14 well)

attributes required by the proposed technique are acoustic impedance (AI) and Poisson ratio.

7. Application of the validated model (Figure 4) on seismic attributes. Provided the needed distributions of seismic attributes are available, porosity and water saturation distributions can be established.
8. Validation of results through analyses on reservoir geological and engineering evidence.

Although the presented methodology is simple and straightforward, its application on real field data may require some improvisation (Widarsono et al., 2001).

In applying the technique to a limestone reservoir EJ field (Figure 5), there are several problems that hinder its immediate use in the interpretation of seismic attributes. The problems are summarized as follows:

1. Unlike the AI attribute (for the top 10 millisecond of the reservoir) that is provided directly from seismic inversion (Figure 6) corresponding Poisson ratio data is absent due to the absence of *amplitude variations with offsets* (AVO) analysis or any data recorded using multi-component receivers. Since there is no such map available from seismic processing, its creation based on log data from all wells is a necessity.
2. Unfortunately, some of the wells do not have complete log suites. This makes it difficult to determine all necessary parameters, i.e. porosity, water saturation, acoustic impedance, and Poisson ratio.

The above two problems in fact cannot be solved by conventional practices, although rock physics theory is well understood. It becomes a necessity to apply more advanced technologies such as artificial neural networks to account for the associated uncertainty.

III. ARTIFICIAL NEURAL NETWORKS

Artificial neural networks (ANNs) are currently the most popular technique in artificial intelligence for advanced signal processing. Given a set of multivariate input and target measurements, ANNs can learn and extract their complex non-linear relationships. The relationships can be applied to estimate the target variables when the actual measurements are not available. Many previous studies have shown encouraging results in field applications, compared with well-established techniques such as multiple linear regression and discriminant analysis (e.g. Wong et al., 1995; Bruce et al., 2000).

The neural networks used in this study are supervised backpropagation networks. Backpropagation is a gradient descent algorithm that is used to estimate coefficients (neural connection strengths) by minimizing an error function (Bishop, 1995).

A. *Prediction of missing log suites*

The immediate problem that must be solved is the absence of some well log data. The most important synthetic log data is the acoustic log (monopole) and density log. Alternatively, missing Poisson ratio values would be required for the generation of Poisson ratio spatial distribution. Also, the missing acoustic impedance, along with the corresponding Poisson ratio values is required for validation purposes, presented later in the process of validation for both AI and Poisson ratio maps.

The presented example uses fourteen (14) wells from the EJ field. Of the 14 wells only five wells have acoustic logs and seven wells have density logs for the estimation of Poisson ratio and AI. These data are important for the generation of Poisson ratio spatial distribution, and for the validation purposes. The missing logs (acoustic and density) are generated from known relationships found in other wells.

Based on a detailed analysis of the well logs in all wells, one of the wells was selected as the key well for the study. The well logs of this well were used as training data. A neural network was setup to predict the missing logs. The types of input logs presented to the neural network were the conventional open-hole well logs, and the output logs were the missing logs (i.e. acoustic and/or density logs). Figure 7 shows an example of the predicted acoustic and density in a candidate well (well EJ-2). The results conformed with the geological setting of the field. The predicted acoustic and density logs were then presented to the corresponding equations derived from rock physics theory for the estimation of both AI and Poisson ratio.

B. *Generation of the Poisson ratio map*

The Poisson ratio data set contains a total of 841 values from fourteen wells. However, many calculated Poisson ratio values were out of the range that is considered typical (0.05 to 0.35) (coals can have Poisson ratios higher than 0.4). This was partly due to physical limitation of the equations when applied to reservoirs with extreme porosity values (too low and too high) and partly due to difference in resolution that characterizes the acoustic and density logs needed for the estimation of Poisson ratio. It is worth noting that two survey tools,

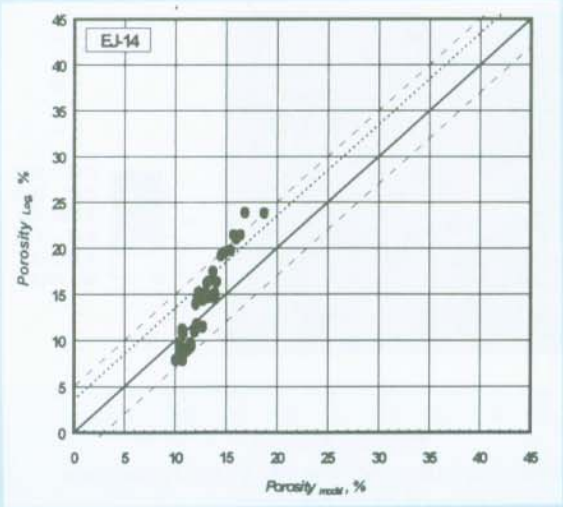

Figure 8
Test for Poisson ratio estimates. Comparison between porosity estimates and porosity from conventional log analysis (EJ-14 well)

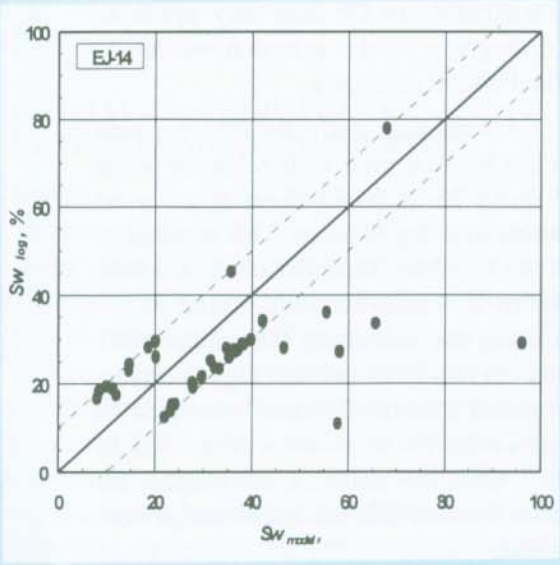

Figure 9
Test for Poisson ratio estimates. Comparison between water saturation estimates and water saturation from conventional log analysis (EJ-14 well)

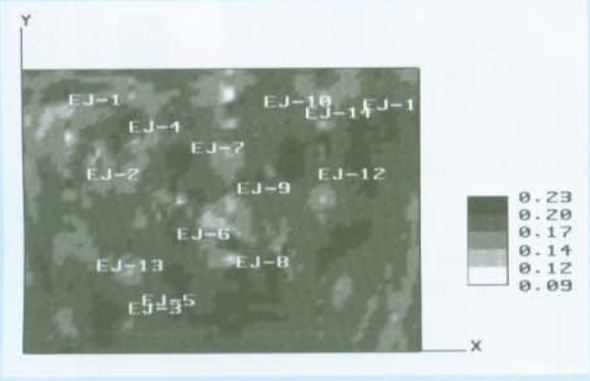

Figure 10
Poisson ratio map for the 10 milliseconds interval of the EJ reservoir

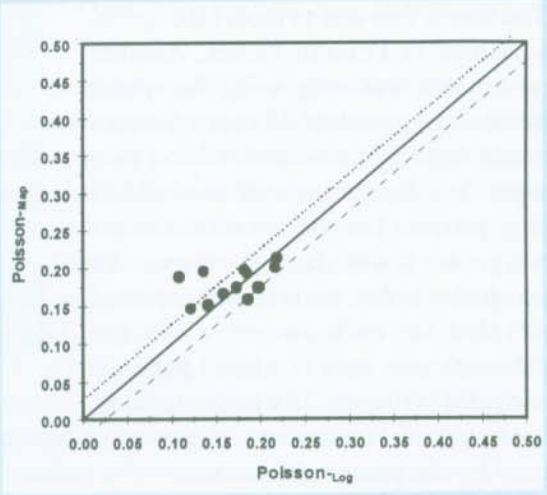

Figure 11
Comparison between Poisson ratio values from map at well locations and average Poisson ratio values from the wells

having different depth of investigation (giving different resolution), operating in highly heterogeneous limestone may produce inconsistencies in the data they produce. Accordingly, a careful selection was made on the Poisson ratio data.

In this separate study, the first step was to select Poisson ratio with values between 0.05 and 0.35, and take them as the most representative log patterns. This resulted in total of 151 values. The second step was then to setup a neural-network aimed at re-estimating the remaining 690 values (841 minus 151) using all the well logs as inputs. A sigmoid transfer function was used to constrain the Poisson values from 0.05 to 0.35. After the network converged, all Poisson values within the desired range were obtained.

The third step was to check the validity of the estimated Poisson ratio data. Poisson ratio estimates and corresponding AI data were input into the model derived previously (Figure 4), and this resulted in porosity and water saturation estimations. The porosity and water saturation estimates were then compared to the porosity and water saturation values produced by conventional log analysis (Figures 8 and 9).

The fourth step was to model the spatial relationships of Poisson values. Another neural network was setup using the spatial coordinates (x,y,z) and the AI values (derived from well logs) as inputs, and Poisson ratio as output. Initially, the network used all 841 training patterns but the iteration did not converge to a satisfactory error. An examination was then made on the individual error value for each pattern. Only the patterns with low errors ("clean" patterns) were selected (410 points) for further training. The inconsistent Poisson ratio values were later to be replaced by the produced estimates.

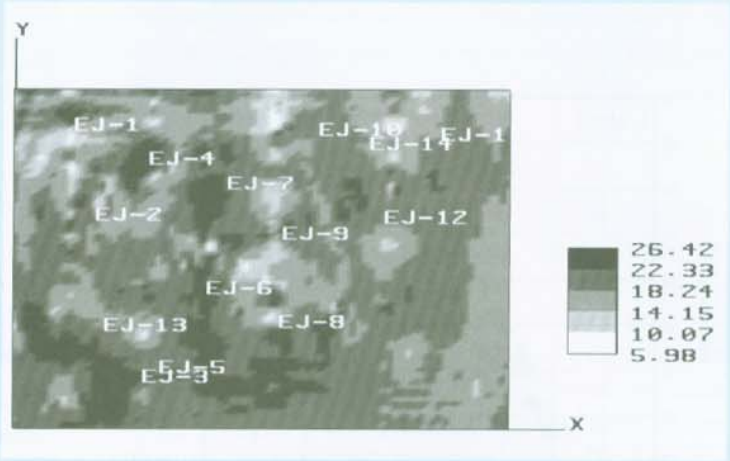

Figure 12
Porosity lateral distribution for the top 10 microseconds interval of EJ reservoir

Figure 12
Water saturation lateral distribution for the top 10 microseconds interval of EJ reservoir

After the removal of the unrepresentative patterns, the network converged and the seismic-derived AI value at each coordinate was presented to the trained network. It is emphasized that this approach used the log-derived AI values to train the networks, followed by the seismic-derived AI values to make subsequent predictions. This is a valid approach in the sense that neural networks provide only approximations to the log-derived AI values during the learning phase. The scaling problem becomes insignificant after the network is trained. Figure 10 shows the Poisson ratio lateral distribution for the top 10 milliseconds travel time (approx. 40 ft) of the reservoir.

In the final step a comparison was made between the predicted Poisson values at the well locations and

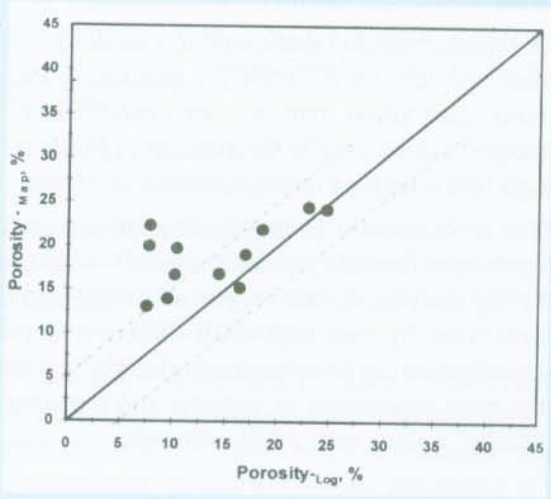

Figure 14
Comparison between porosity values from map at well locations and average porosity values from the wells

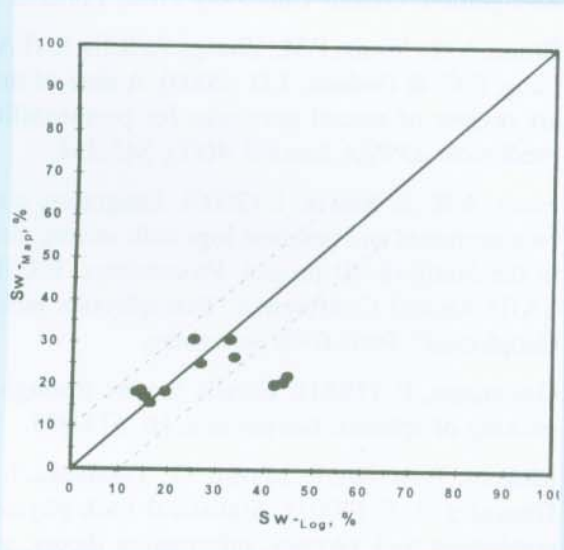

Figure 15
Comparison between water saturation values from map at well locations and average water saturation values from the wells

the average Poisson ratio values of the wells for the particular interval. The results were satisfactory, except for wells with very low porosity values (wells EJ-12 and EJ-13), which were lower than the engineering *cut-off* value of 7%; (Figure 11).

IV. SPATIAL DISTRIBUTION OF PETROPHYSICAL PROPERTIES

Initially, it was planned that as AI and Poisson ratio data became available then the distributions of porosity and water saturation would be established through the use of the correlation presented in Figure 4. However, it was later thought that it would not produce any significant new information since the training patterns that were used in the generation of Poisson ratio have already been strictly controlled by the correlation in Figure 4. The provision of the porosity and water saturation distribution was then assigned to neural networks with the selected log data used as the training patterns, and the AI and Poisson ratio spatial distributions (Figures 6 and 10) as input data for the resulting trained network. The porosity and water saturation distribution for the area of interest is presented in Figures 12 and 13, respectively.

In judging the validity of the porosity and water saturation maps, two approaches were taken. Firstly, a well-based approach was taken, to check the agreement between predicted values at well locations and the average values form log analysis for the relevant wells. Secondly, a macro approach was used to check the soundness of the maps from the point of view of reservoir geology.

Figures 14 and 15 respectively present the comparison between map and average well values for all wells (except well EJ-3 which is dry hole). In general, the agreement seems satisfactory except for some wells that are characterized by low porosity (wells EJ-12 and EJ-13). This is indicated by plots, which show that most data fall within the 3-porosity unit (pu) envelope (Figure 14) and 10 percent water saturation envelope (Figure 15). As stated earlier, the exclusion of porosity and water saturation data from wells EJ-12 and EJ-13 is considered justified since much of this data has been excluded from the training patterns due to inconsistencies discussed earlier. However, one marked consistency is shown by causality between the two variables in which water saturation tends to be high for low porosity low for high porosity. This correlation, which can be demonstrated petrophysically, shows that the neural network output is consistent with the input data.

A second approach in assessing the reliability of the porosity and water saturation maps (Figures 12 and 13) is through geological consideration. It is commonly acknowledged that lateral porosity variations in carbonate reservoirs are very difficult to determine. As stated by Murray (1960), porosity in carbonate rocks results from many processes, both depositional and post-depositional, and is dictated largely by the history of the rocks themselves. Considering the complexity of porosity in carbonates, it is therefore difficult to assess the validity of porosity maps, without detailed studies of the origin of the porosity in the EJ reservoir. The porosity map is consequently not included in the evaluation.

Evaluation of the water saturation map (Figure 13) is easier to conduct than the evaluation of porosity map. By comparing top-structure map (Figure 5) and the water saturation map, a similarity is visible. The most notable consistency is the presence of oil-water contact in the southeast corner of the study area, indicated by the presence of higher water saturation upon which is separate from areas of lower water saturation. Indeed, it is worth noting that considering the estimated water saturation cut-off value of 60% the highest water saturation value of roughly 44% (Figure 15) appears to be too optimistic. This bias is probably caused by the validity of the model as it is applied throughout the reservoir as well as by the validity of Gassmann model itself in the case of non-clastic limestone reservoir. Considering the modeling is conducted in one key well only, inclusion of more wells representing different locations may yield better results. Nevertheless, considering the potential error of 10–20 percent of pore space, depending on the reliability of log data and problems encountered, often found in water saturation values derived from log analysis the water saturation map in Figure 13 can still be regarded as a reasonably good and reliable result.

V. CONCLUSIONS

A series of conclusions has been drawn from the study:

- An intelligent approach to help determining rock physical properties from seismic data has been proposed. However, improvisation may have to be used depending on data availability.
- The use of rock physics theories ("hard computing") has benefited much from the intelligent approach ("soft computing") in the form of artificial neural networks (ANNs). The use of ANNs could be more intensive in cases that need the ability to learn patterns of other variables, such as rock matrix density and shale content.
- A separate method that combines modeling of log data and the use of ANN for generating Poisson ratio distribution map has been established. The method can be used in the absence of Poisson ratio data that is derived through seismic inversion.
- The application of an intelligent approach is useful for solving intrinsic problems normally encountered by log analysts. As shown, potential inconsistencies exhibited by two logs with different depth of investigation can be reduced significantly by selecting the most representative patterns and replacing the "faulty" values with ANN estimates.

VI. ACKNOWLEDGMENT

The authors thank Mr. Eddy Mujiono, Ms. Rosjati Noor, and Mr. Bambang A. Wijayanto from the Exploitation Division, LEMIGAS, for their technical support during the study.

REFERENCE

1. Bishop, C.M. (1995). *Neural Network for Pattern Recognition*, Oxford University Press, London.
2. Bruce, A.G., Wong, P.M., Zhang, Y., Salisch, H.A., Fung, C.C. & Gedeon, T.D. (2000). A state-of-the-art review of neural networks for permeability prediction. *APPEA Journal*, 40(1), 343-354.
3. Furre, A.K. & Brevik, I. (2000). Integrating core measurements and borehole logs with seismic data in the Statfjord 4D project. Proceedings, EAGE-SAID Annual Conference "Petrophysics meets Geophysics", Paris 6 - 8 November.
4. Gassmann, F. (1951). Elastic waves through a packing of spheres. *Geophysics*, 16, 673-685.
5. Mukerji, T. Avseth, P., Mavko, G., Takahashi, I. & Gonzalez, E.F. (2001). Statistical rock physics: combining rock physics, information theory, and geostatistics to reduce uncertainty in seismic reservoir characterization. *The Leading Edge*, March, p: 313 – 319.
6. Murray, R.C. (1960). Origin of porosity in carbonate rocks. *Journal of Sedimentary Petrology*, 30(1), 59-84.

7. Vidal, S., Longuemare, P., Huguet, F. & Mechler, P. (2000). Combining geomechanics and geophysics – a need for reservoir seismic monitoring. Proceedings, EAGE-SAID Annual Conference "Petrophysics meets Geophysics", Paris 6 - 8 November.

8. Widarsono, B. & Saptono, F. (1997). Acoustic measurement in laboratory: a support in predicting porosity and fluid saturation from seismic survey. (in Bahasa Indonesia) Proceedings, Symposium and 5th Congress of Association of Indonesian Petroleum Experts (IATMI), Jakarta.

9. Widarsono, B. & Saptono, F. (2000a). A new method in preparing laboratory core acoustic data for assisting seismic-based reservoir characterization. Proceedings, extended abstract presented at the 2000 Symposium of Society of Core Analyst (SCA/SPWLA), Abu Dhabi.

10. Widarsono, B. & Saptono, F. (2000b). A new approach in processing core and log data for assisting seismic-based mapping of porosity and water saturation. Proceedings, presented at the 2000 EAGE Conference, "Petrophysics meets Geophysics", Paris.

11. Widarsono, B. & Saptono, F. (2001). Estimating porosity and water saturatiom from seismic/acoustic signals: A correction on the effect of shaliness, *Lemigas Scientific Contributions*, no.1/2001.

12. Wong, P.M., Taggart, I.J. & Jian, F.X. (1995). A critical comparison of neural networks and discriminant analysis in lithofacies, porosity and permeability predictions. *Journal of Petroleum Geology*, 18(2), 191-206. •